

PAPER • OPEN ACCESS

## Validation of relations for the determination of pyrotechnic igniter mass

To cite this article: A Salama *et al* 2020 *IOP Conf. Ser.: Mater. Sci. Eng.* **973** 012004

View the [article online](#) for updates and enhancements.

You may also like

- [Experimental study on energy characteristics and ignition performance of recessed multichannel plasma igniter](#)  
Bang-Huang Cai, , Hui-Min Song et al.
- [Tests of igniter's charge position influence on ballistic parameters of artillery rounds](#)  
A Plachá and K Hipnarowicz
- [Application study on plasma ignition in aeroengine strut-cavity-injector integrated afterburner](#)  
Li FEI, , Bingbing ZHAO et al.



**ECS**  
The  
Electrochemical  
Society  
Advancing solid state &  
electrochemical science & technology

**DISCOVER**  
how sustainability  
intersects with  
electrochemistry & solid  
state science research

# Validation of relations for the determination of pyrotechnic igniter mass

**A Salama<sup>1</sup>, H Belal<sup>2</sup> and H M Abdalla<sup>3</sup>**

<sup>1</sup> M.Sc. Student, Rocket Department, Military Technical College, Egypt.

<sup>2</sup> Assistant Professor, Rocket Department, Military Technical College, Egypt

<sup>3</sup> Associate Professor, Rocket Department, Military Technical College, Egypt.

hbelal@mtc.edu.eg

**Abstract:** Propellant ignition is an essential process in solid rocket motor operation as it is responsible of starting the combustion and to reliably self-sustain burning of the solid propellant. Despite the importance of igniter design and ignition process, the relations dealing with igniter mass determination are not well studied and not validated against actual motors with a systematic variation of parameters. The main objective of the current research is to validate the available equations in open literature for determination of the mass of igniter pyrotechnic charge. Data from seven real solid propellant rocket motors were used to validate the relations. These motors have different sizes, grain geometries and pyrotechnic compositions. The results show that the equation of Brayon–Lawerene has the smallest root mean square error (RMSE), and so, it is considered more convenient.

## 1. Introduction

Propellant ignition is an essential process for starting a solid propellant rocket motor. It can be simply defined as a fast and high heat release accompanied by large gas amount per unit mass of the igniter charge to raise the temperature of the propellant surface above the self-ignition temperature and partially raise the pressure in the motor free volume above the low deflagration limit for the propellant [1]. The ignition process is a complicated process, figure 1, which consists of different paths to transfer energy between different phases. The main problem is the failure to start the rocket motor or to reach the self sustaining state due to insufficient heat energy produced by the igniter. Many accidents have been encountered, caused by ignition failures as in the 3<sup>rd</sup> stage of Ariane-2 at 1986 [2] and in the 2<sup>nd</sup> stage Zefiro 23 motor of the Vega rocket at 53 km altitude.

There are two main types of igniters: pyrogen and pyrotechnics igniters [3]. Pyrogen igniter, figure 2, can be considered simply as a small rocket motor used to ignite a larger motor. It is not designed to generate thrust and its major objective is to produce sufficient energy output to ignite a large scale rocket motor. The igniter has to be kept as small and light as possible, and could have one or more nozzles; in most cases its nozzle is subsonic. The pelleted pyrotechnic [5] igniter, figure 3, uses a solid energetic material to ignite the solid rocket motor. Pyrotechnics give a large amount of energy at a very small time. With a proper design, no shockwave will be produced which results in avoiding pressure spikes during the ignition that may affect the propellant mechanical properties [6]. Different pyrotechnic compositions are used for the igniter, and their relevant properties are listed in table 1.



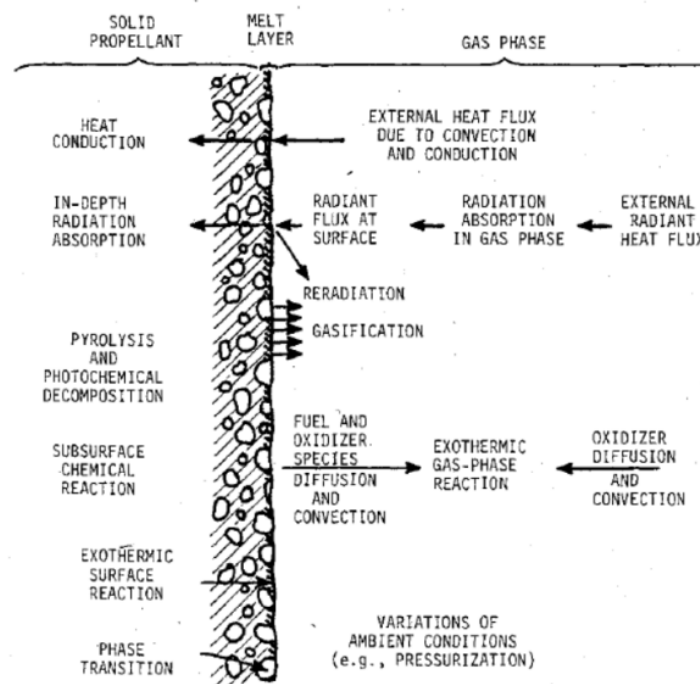


Figure 1. Physical processes involved in solid propellant ignition [4].

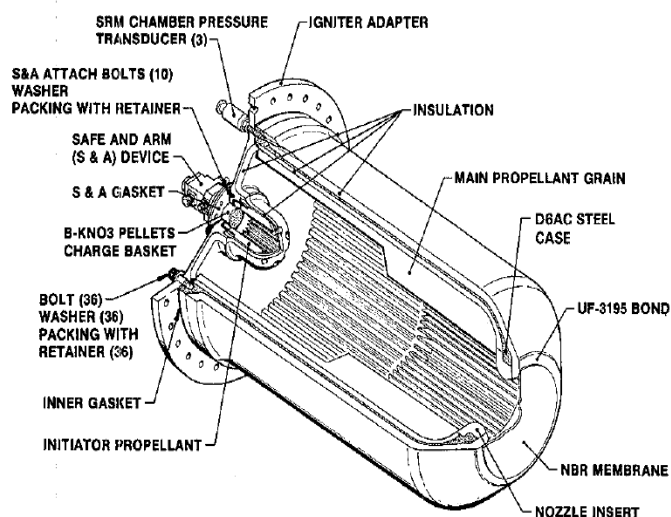


Figure 8. SRM Igniter

Figure 2. Pyrogen igniter [3].

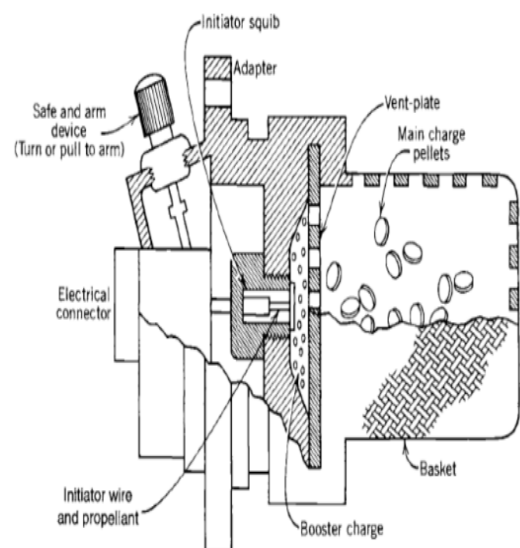


Figure 3. Pyrotechnic igniter [3].

**Table 1.** Main Pyrotechnic Composition Characteristics [7].

| Composition   | Heat of Combustion (cal/gram) | Burning rate at 1 atm (mm/s) | Characteristics   |
|---|-------------------------------|------------------------------|---|
| <b>Black powder:</b><br>75% KNO <sub>3</sub> ,<br>15% charcoal,<br>10% sulfur | 755                           | 28.95                        | -Granular or consolidated configurations, figure 4.<br>-Ease to ignite but produce low energy.<br>-Quench at high altitudes,<br>-Used in: C-5 57mm, SNEP 68mm, FROG-7 rockets |
| <b>BKN</b><br>80% KNO <sub>3</sub> ,<br>19% B,<br>1% wax                      | 1550                          | 9.9                          | -Pellet form<br>-Ease to ignite at low pressure and high altitudes.<br>-High gas content<br>-Used in Minuteman missile igniter.   |
| <b>MTV:</b><br>Magnesium,<br>Teflon,<br>Viton<br>(MTV)                        | 2200                          | 1.778                        | -Produce high energy.<br>-Low hygroscopicity.<br>-Low temperature and pressure dependence<br>-Hard to ignite<br>-Used in Pershing missile igniter, figure 5.                  |

**Figure 4.** Black powder [8].**Figure 5.** Magnesium/Teflon/Viton Pellet [9].

Five possibilities for the ignition pressure-time curve are shown in figure 6. The curves A and E represent a misfire for two contradictory reasons. The curve A shows a high energy release in a very short time. The misfire curve E is attributed to the heat being released through a very long ignition delay.

The factors affecting this ignition delay time are numerous. For example: imperfection in squib current, igniter charge temperature, pyrotechnic characteristics, charge packing or moisture may affect ignition time delay [8]. The curve B shows the ignition spike, giving an indication of over-weighted pyrotechnic charge. The curve (c) represents the proper pressure time ignition curve, while the curve D indicates a hang-fire as it failed to reach a self-sustained state. Figure 7 shows “*the ignition corridor*” [9] state in a logarithmic scale between ignition time and ignition energy represented in radiant flux. It is evident from the figure that start of combustion of solid propellant does not mean reaching to the sustained state. This ignition corridor defines the limits of energy imparted to propellant surface in order to get propellant ignited. As indicated in figure 4 lower values lead to case E while higher values lead to case A or “*over-driven combustion*”.

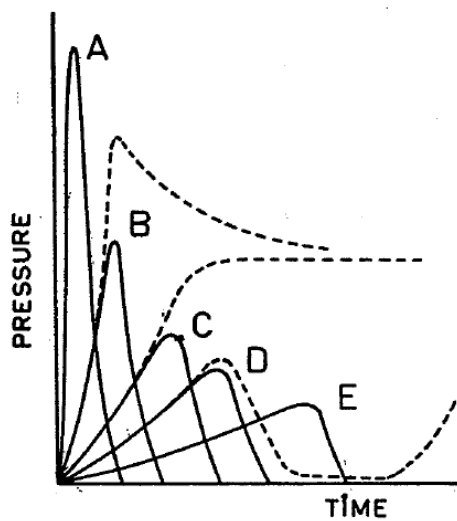


**Figure 6.** Possible pressure-time curves during ignition [6].

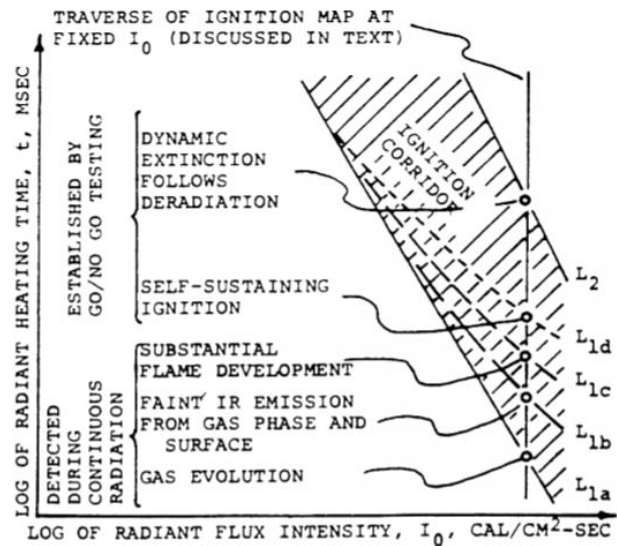


**Figure 7.** Ignition corridor [9].

## 2. Ignition charge mass equations

As it is discussed previously, ignition process is a complicated process, it is too hard to get analytical solution for the pyrotechnic mass required and hence all the equations available are empirical. The main contribution in this research is to validate these equations against real igniters in order to grip the main factors affecting the ignition process which may help acquire a better igniter design. Three empirical equations will be handled in the following sections.

### 2.1. Free Volume Equation [5]

In this relation the required mass depends only on free volume of the combustion chamber including the convergent section. This equation was developed based on more than 15 different rocket motors with varying propellant formulation, free volume, igniter composition and grain configuration, figure 8.

$$m_{ig} = 0.016944 (V_c)^{0.7} \quad (1)$$

$m_{ig}$ .....pyrotechnic charge mass, gram.

$V_c$ .....combustion chamber free volume including the convergent section,  $\text{cm}^3$ , figure 9.

### 2.2. Brayon-Lawerene equation [10]

This relation depends on calculating the total energy required to ignite propellant surface taking in consideration the thermodynamic properties of the propellant, the grain length and the total area exposed to ignition. This equation was developed based on 53 different rocket motors with varying propellant formulation, igniter composition and grain configuration, This equation states that:

$$Q = 38 \left[ A_s q_c \left( \frac{L_g}{A_s} \sqrt{4\pi A_p} \right)^{0.59} \right]^{1.06} \quad (2)$$

where

Q total energy required for ignition, cal.

- $A_s$  total area exposed to igniter products, figure 10, including the burning surface of propellant grain, the convergent area of combustion chamber, inhibited area of grain end and any other solid parts like grids,  $\text{cm}^2$ .
- $q_c$  experimental ignition energy per unit area of propellant,  $\text{cal}/\text{cm}^2$ .
- $L_g$  propellant grain length,  $\text{cm}$ .
- $A_p$  cross-sectional port area,  $\text{cm}^2$ .

The igniter mass can be calculated by defining the pyrotechnic charge composition and determination of its combustion heat using equation 3.

$$Q = m_{ig} \Delta H_{comb} \quad (3)$$

where

- $m_{ig}$  mass of igniter, gm.
- $\Delta H_{comb}$  heat of combustion of igniter material,  $\text{cal}/\text{gram}$ . Calculated by NASA (CEA) [13] thermochemical calculations.

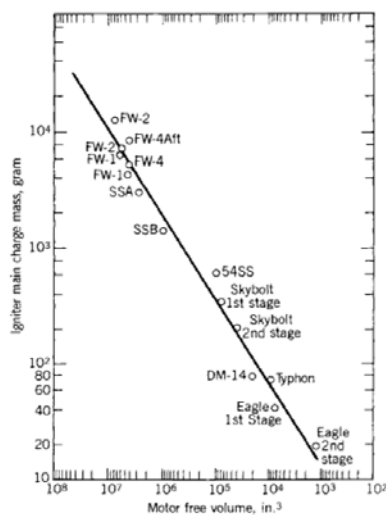


**Figure 8.** Igniter pyrotechnic charge weight to motor free volume [5].

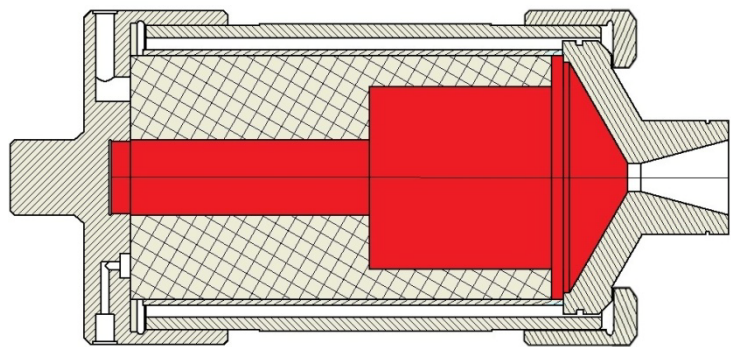


**Figure 9.** Free volume of combustion chamber (red volume).



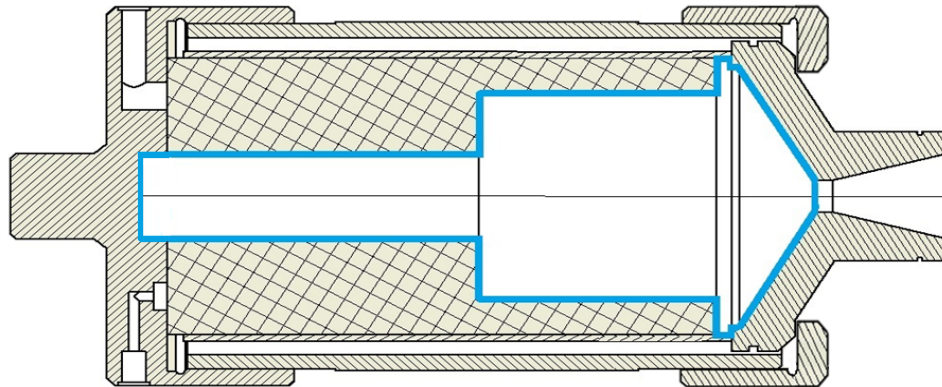


**Figure 10.** Area exposed including the grain surface inhibited surface and the convergent section.

### 2.3. Ideal gas equation [6]

This relation is based on the ideal gas law, it depends on different parameters: the initial free volume of the combustion chamber, the ignition pressure, isochoric temperature and the solid fraction in the combustion gases. The propellant and pyrotechnic properties are neglected

$$m_{ig} = \frac{1}{1-\varepsilon} \frac{P_{ig} V_{ig}}{\frac{R_u}{M} T_{ig}} \quad (4)$$

where

|               |  |
|---------------|--|
| $m_{ig}$      | calculated mass of ignition charge, kg.                                  |
| $V_{ig}$      | free ignition volume, m <sup>3</sup> .                                   |
| $\varepsilon$ | fraction of condensed phase in combustion products of ignition charge,   |
| $R_u$         | universal gas constant, J/(mol-K);                                       |
| $M$           | molar mass of combustion gas of ignition charge, kg/mol.                 |
| $T_{ig}$      | combustion gas temperature of ignition charge, K.                        |
| $P_{ig}$      | ignition pressure or the lower deflagration pressure, N/m <sup>2</sup> . |

Lower deflagration pressure is the minimum value for combustion chamber pressure to sustain the propellant combustion [11]. For double base propellant, it often has a value above 30 bar and for ammonium perchlorate based composite propellant it has a lower value above 20 bar [12], in spite of the fact that composite propellant is slightly more difficult to ignite than double base propellant [6].

### 3. Case studies

In order to validate the previous equations, the three equations are used to calculate the igniter mass for different motors. Most of these motors use double base propellant. The motors have a huge difference in size, table 2. Calculated igniter charge masses values are compared with those from real motors. In this study, different types of pyrotechnic charge with different compositions were used:

- Black-powder with composition Sulfur S 10%, Charcoal C 15%, potassium nitrate KNO<sub>3</sub> 75%.
- SR 371C with composition Magnesium Mg 42%, potassium nitrate KNO<sub>3</sub>, with acaroid resin binder [8]

The thermochemical characteristics for these types were calculated by NASA (CEA) [13] to get the required parameters.

**Table 2.** Case study motors.

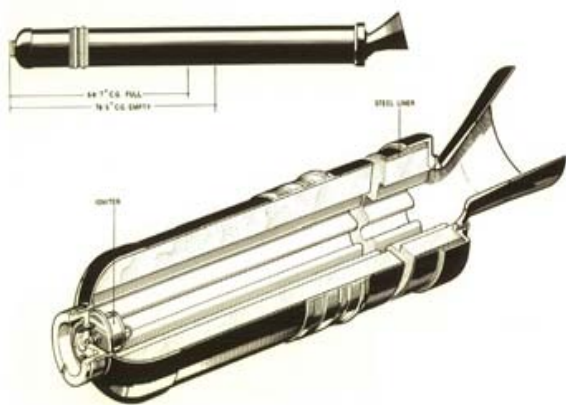
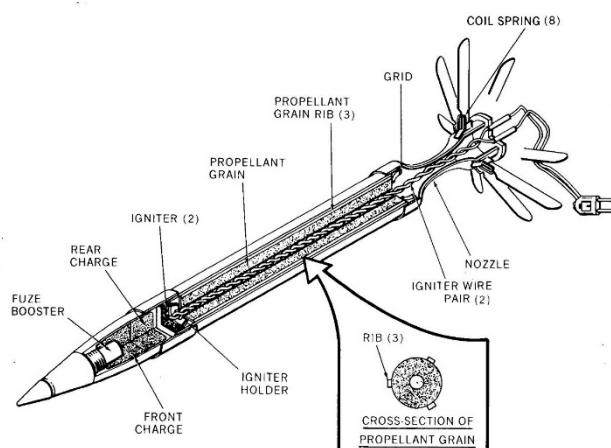
|         | Free volume<br>(cm <sup>3</sup> ) | Area exposed $A_s$<br>(cm <sup>2</sup> ) | $A_s / A_p$ | Grain length<br>(cm) |
|---------|-----------------------------------|--|-------------|----------------------|
| Motor 1 | 207                               | 165.82                                   | 322         | 45                   |
| Motor 2 | 1100000                           | 133012.23                                | 158         | 474                  |
| Motor 3 | 748                               | 273.53                                   | 213         | 42.6                 |
| Motor 4 | 129089                            | 90980.02                                 | 716         | 115                  |
| Motor 5 | 220683                            | 152956.85                                | 763         | 173.1                |
| Motor 6 | 4058                              | 3066.12                                  | 2310        | 89                   |
| Motor 7 | 37165                             | 17806.49                                 | 138         | 287.                 |

#### 4. Results and discussion

The results of applying the three relations on motors in the case studies are shown in table 3. Comparison between the actual and calculated igniter masses using equations 1 through 3 are shown in figures 13-15 respectively. The following analysis can be drawn:

**Table 3.** Igniter pyrotechnic charge mass.

|         | Actual mass<br>(gram) | Equation 1<br>(gram) | Equation 2<br>(gram) | Equation 3<br>(gram) |
|---------|-----------------------|----------------------|----------------------|----------------------|
| Motor 1 | 5                     | 0.71                 | 3.30                 | 3.25                 |
| Motor 2 | 5066.4                | 287.08               | 2661.83              | 6476.84              |
| Motor 3 | 5.9                   | 1.74                 | 5.28                 | 1.17                 |
| Motor 4 | 3024                  | 64.07                | 511.57               | 2027.70              |
| Motor 5 | 5040                  | 93.25                | 949.42               | 3466.43              |
| Motor 6 | 63                    | 5.69                 | 23.61                | 63.74                |
| Motor 7 | 100                   | 26.80                | 77.61                | 136.75               |

**Figure 11.** Motor No.7 [14].**Figure 12.** Motor No. 1 [15].

- Results from the first equation underestimated the igniter mass charge in all the cases. The best match was observed for the composite motor based on AP. This might be explained by the fact that this empirical equation was originally proposed for composite propellant [5].



- The second equation gives a slightly better result, especially with small scale motors. A larger scale motor has a large burning area, which justifies the notable discrepancy between actual and calculated pyrotechnic masses.
- For the third equation; a large deviation is observed for small motors.
- To have a quantitative judgement on the prediction of each equation, a root mean square error (RMSE) is calculated according to the following equation

$$\text{RMSE} = \sqrt{\frac{\sum \left(1 - \frac{m_{\text{calculated}}}{m_{\text{real}}}\right)^2}{n}} \quad (5)$$

where

$m_{\text{cal}}$  the calculated igniter charge mass  
 $m_{\text{real}}$  the real igniter mass value  
 $n$  the total number of studied motors

On reviewing the pressure time curve for each motor, a presence of an ignition spike was observed, which gives a direct indication for an over-weighted igniter charge. This phenomenon was highly pronounced in motors 4, 5 and 6 as shown in figures 16-18. In motor #4 a pressure spike of 140 bar is noticed while the average pressure was targeted to be 70 bar; this implies that the igniter charge mass was nearly twice the proper value. Similarly, the figures show for the motor 5 an ignition spike of 110 bar and a steady state pressure of 60 bar, while for the motor 6, an ignition spike of 130 bar and steady state pressure 85 bar.

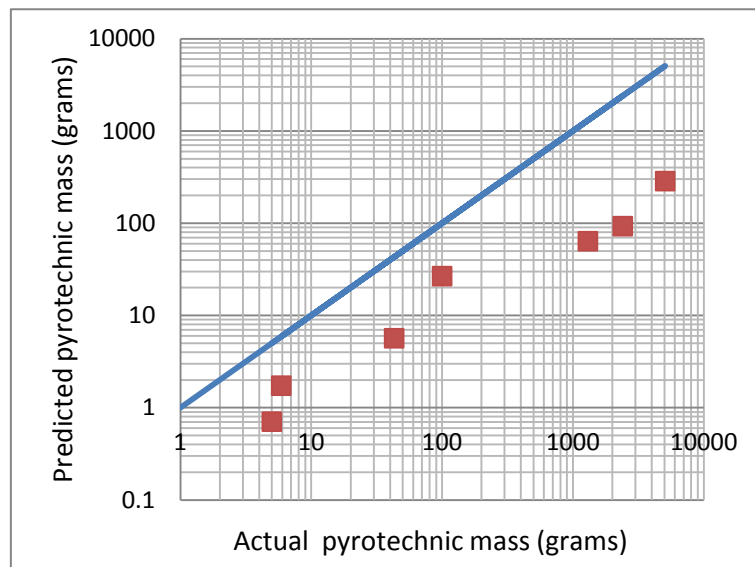


**Figure 13.** Comparison with results from equation 1.

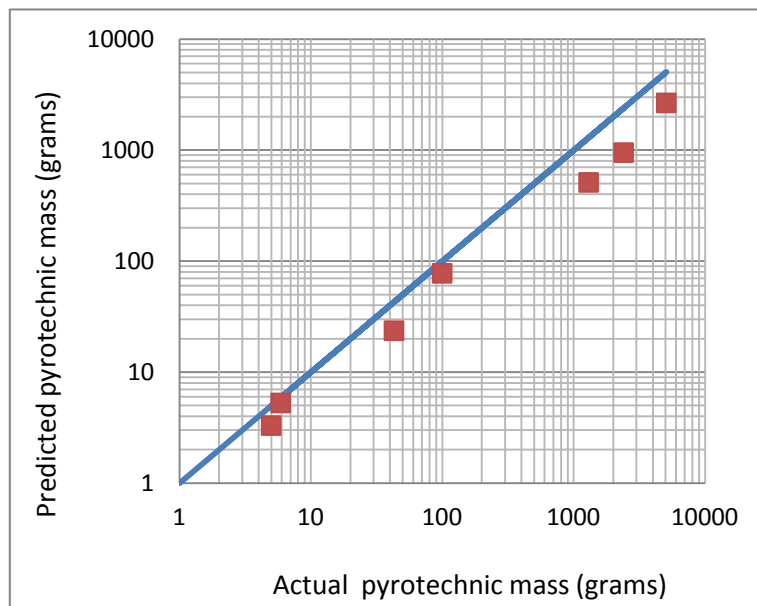


**Figure 14.** Comparison with results from equation 2.

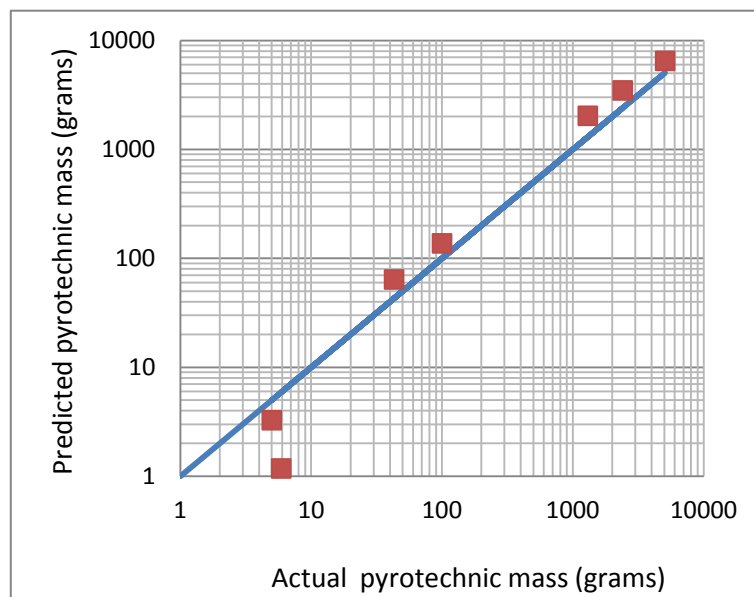


**Figure 15.** Comparison with results from equation 3.

Results are shown in table 4.

**Table 4.** Root mean square error.

|            | Root mean square error (%) |
|------------|----------------------------|
| Equation 1 | 88                         |
| Equation 2 | 55                         |
| Equation 3 | 41                         |

To remove spikes in the pressure-time curves it was necessary to modify the ignition masses for the motors 4, 5 and 6. The motors were fired with “*modified real values*” and no such spikes, were recorded. A comparison between the original values and “modified real values”. versus re-calculated RMSE values are shown in table 5.

**Table 5.** Corrected igniter pyrotechnic masses.

|         | Original mass<br>(gram) | Corrected mass<br>(gram) |
|---------|-------------------------|--------------------------|
| Motor 4 | 3024                    | 1300                     |
| Motor 5 | 5040                    | 2400                     |
| Motor 6 | 63                      | 43                       |

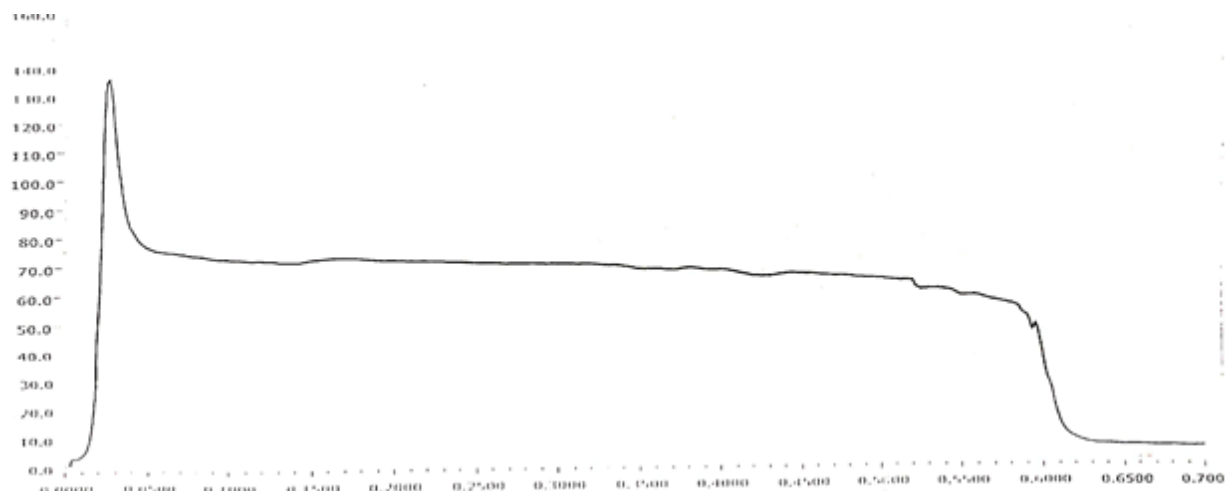


**Figure 16.** Pressure time curve for motor no.4

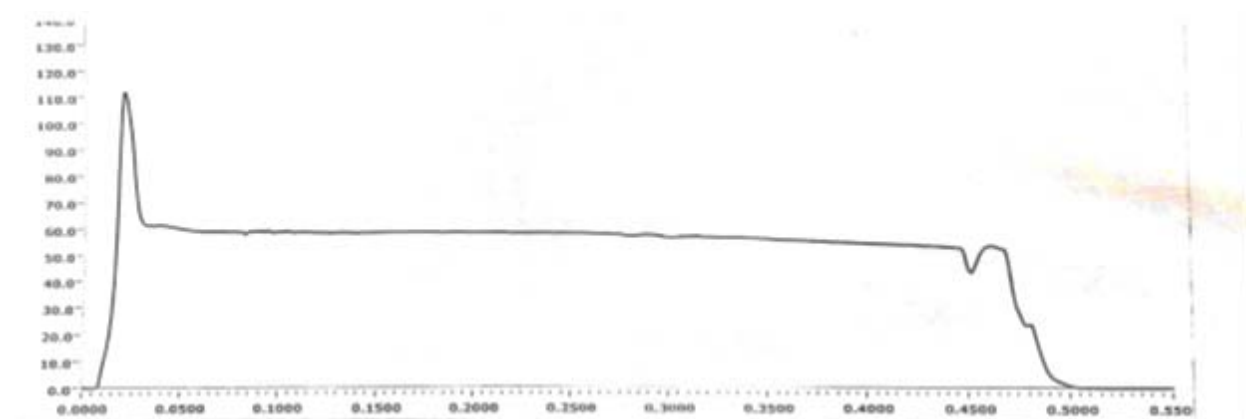


**Figure 17.** Pressure time curve for motor no.5

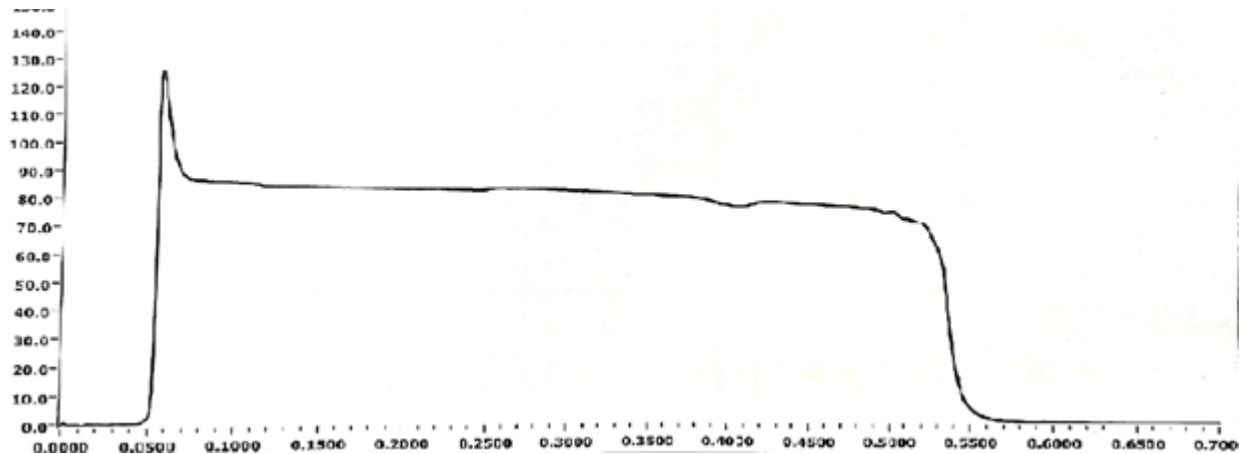


**Figure 18.** Pressure time curve for motor no.6.

After correcting the igniter pyrotechnic mass according to the pressure time curve of each motor the igniter pyrotechnic mass were changed and the results are shown in Figs 19, 20, 21.

- The first equation still has a large deviation between the calculated result and the real pyrotechnic mass,
- For the second equation the result is under estimated after the correction but the results make a better sense with the correcting masses.
- the third equation also give a better fitting with the correcting masses except motor number 1

Now the second equation give the minimum root square and the best fitting data and the third equation go a little higher by about 10%.

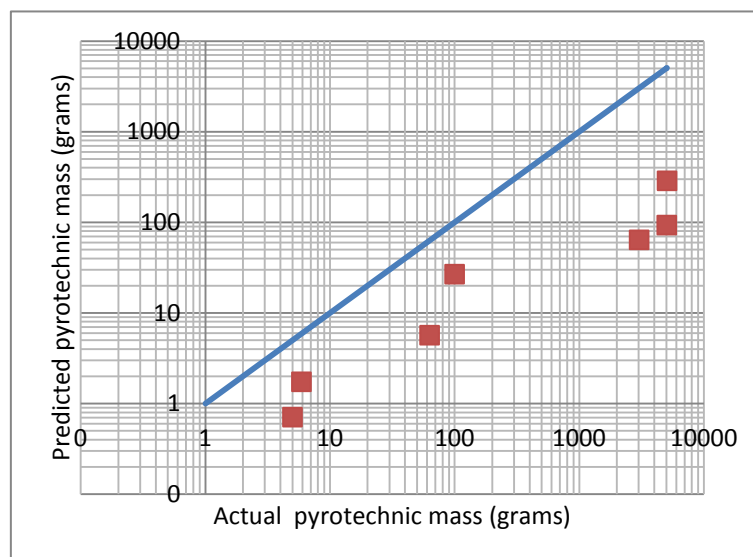


**Figure 19.** Equation 1 result vs. the corrected pyrotechnic igniter mass.

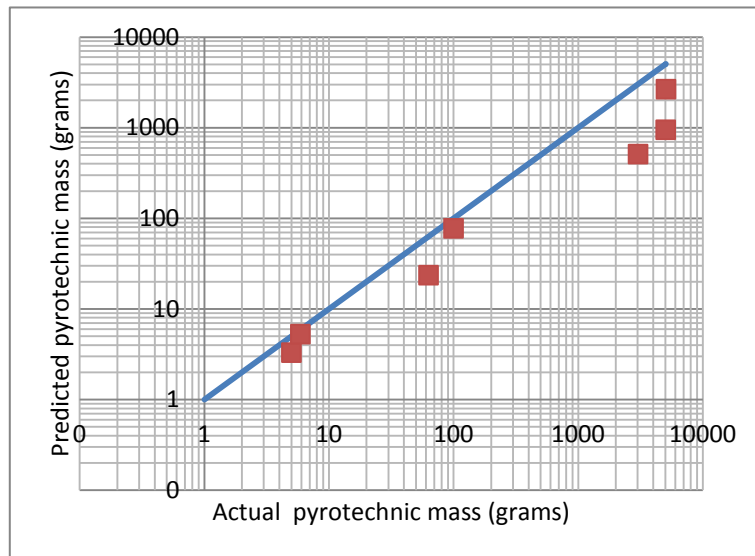


**Figure 20.** Equation 2 result vs. the corrected pyrotechnic igniter mass.

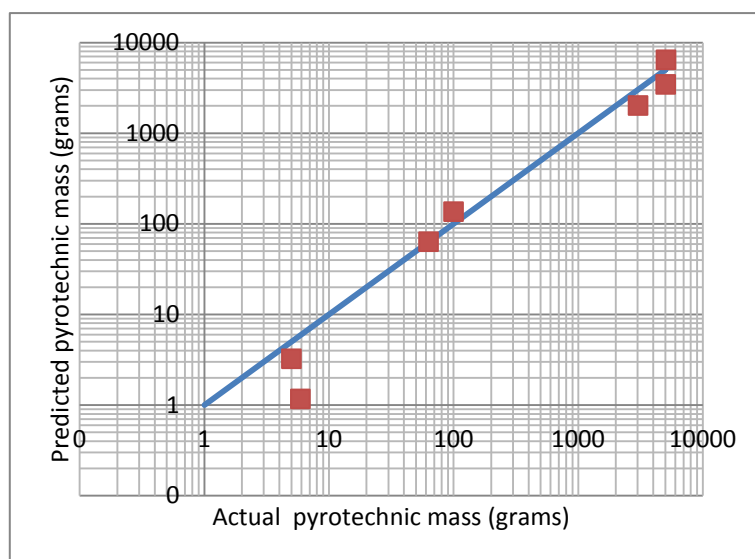


**Figure 21.** Equation 3 result vs. the corrected pyrotechnic igniter mass.

**Table 6.** Corrected- Root mean square error

|            | Root mean square<br>Error (%) | Corrected Root mean<br>square errors (%) |
|------------|-------------------------------|--|
| Equation 1 | 88                            | 89                                       |
| Equation 2 | 55                            | 43                                       |
| Equation 3 | 41                            | 49                                       |

## 5. Conclusion

The equation of Brayon–Lawerene gives less root mean square error than other relations. Therefore, it could be considered more realistic as compared to other equations. The better resulting estimation could be argued to considering wider range of parameters as the exposed area, which is a dominant factor, the energy required for ignition of unit area of propellant, and the produced combustion energy from the igniter pyrotechnic. However, the effects of solid particles within the igniter gas products, the temperature and pressure evolving from these products have been neglected. The free volume equation is too simple as it considers only the effect of combustion chamber free volume, while neglecting the effects of composition and thermodynamic properties of propellant or even the pyrotechnics. The ideal gas equation takes into consideration the igniter composition and the free volume but it neglects composition and properties of the propellant except the deflagration pressure limit. However, all these equations did not consider neither the ignition moment nor the proper ignition delay that may affect the calculated ignition mass. As a future work, it is planned to finely tune Brayon–Lawerene equation through considering the effects of pyrotechnic charge particle size, the presence of solid phase in products, in addition to the relation between estimated mass and motor ignition delay.

## References

- [1] Von Elbe G 1966 Solid propellant ignition and response of combustion to pressure transients *2<sup>nd</sup> Propulsion Joint Specialist Conference* p 668
- [2] Chang, I-Shih, Susumu Toda, and Seishiro Kibe 2000 European space launch failures *36<sup>th</sup> aiaa/asme/sae/asee joint propulsion conference and exhibit*
- [3] Keller jr, r B 1971 *Solid rocket motor igniters NASA SP-8051*
- [4] Kulkarni, Anil k Mridul Kumar, and Kenneth K Kuo 1982 Review of solid-propellant ignition Studies pp 243-244
- [5] Sutton George P; Biblarz O 2016 *Rocket Propulsion Elements* John Wiley & Sons
- [6] Barrere, Marcel, et al. 1960 *Rocket propulsion*. LTAS
- [7] Robertson W 1972 Igniter material considerations and applications *8th Joint Propulsion Specialist Conference*
- [8] Wimpers R 1950 *Internal Ballistics of Solid-fuels Rockets*. New York: mcgraw-Hill
- [9] Deluca l, Caveny L, Ohlemiller T and Summerfield M 1976 Radiative ignition of double-base propellants. I-Some formulation effects *AIAA Journal* 14(7) pp 940-946
- [10] Bryan, George J, and Evan K 1959 A method for predicting ignition energy requirements of Practical propellant systems. part 3 rockets *Naval ordnance lab white oak md*
- [11] Zanutti C; Giuliani P 1994 Pressure deflagration limit of solid rocket propellants: experimental results *Combustion and flame* 98 1-2 pp35-45.
- [12] Atwood A et al. 2009 Radiant ignition studies of ammonium perchlorate based propellants *Progress in Propulsion Physics* 1 pp121-140.
- [13] McBride B, and Gordon S 1996 Computer program for calculation of complex chemical equilibrium compositions and applications ii *User's manual and program description, NASA reference pub. 1311* 1996.
- [14] White C 1960 The development of the gosling ii solid propellant rocket motor *Rocket propulsion establishment wescott (united kingdom)*
- [15] [https://en.m.wikipedia.org/wiki/S-5\\_rocket#/media/File%3AS-5\\_57mm\\_rocket\\_cross-section](https://en.m.wikipedia.org/wiki/S-5_rocket#/media/File%3AS-5_57mm_rocket_cross-section.JPG). JPG retrieved 1<sup>st</sup> Dec 2019